LINKING CSF TO DRAINAGE TIME DURING HANDSHEET FORMATION: REFINING EFFECTS ACROSS WOOD AND NON-WOOD PULPS

NISHI K. BHARDWAJ

Department of Paper and Packaging Technology, Indian Institute of Technology Roorkee, Saharanpur Campus, Saharanpur – 247001, Uttar Pradesh, India
✉ *Corresponding author: nishi.bhardwaj@pt.iitr.ac.in*

Received October, 2025

This study investigates how refining alters drainage behavior during laboratory handsheet formation across five bleached pulps – hardwood, softwood, bamboo, wheat straw, and bagasse – over freeness ranges representative of approach-flow and wet-end operation. For each pulp and refining level, Canadian standard freeness (CSF) and handsheet drainage time (t) were measured and regressed using three compact models: (i) $t = a + b/CSF$, (ii) $\sqrt{t} = a + b.\log(CSF)$, and (iii) $\log t = a + b.\log(CSF)$. All pulps showed the expected increase in drainage time with decreasing CSF, but the rate and curvature were pulp-specific. Transformed models generally outperformed or matched the reciprocal form, with the $\sqrt{t}$-log(CSF) and log–log power laws yielding higher R^2 and lower RMSEE, especially for bamboo and non-wood pulps. Wheat straw exhibited near-perfect fits under $\sqrt{t}$-log(CSF), while bagasse remained the most challenging, reflecting fines/pith effects. The results deliver practical equations for predicting drainage time from CSF within observed ranges and highlight that model choice should be pulp-dependent for reliable dewatering control.

Keywords: pulp refining, Canadian standard freeness (CSF), drainage time, handsheet formation, non-wood fibers (bamboo, bagasse, wheat straw), predictive modeling

INTRODUCTION

Removing water from fiber suspensions is a rate-limiting step in papermaking. It governs machine speed, energy use, sheet formation, and – ultimately – paper properties. Two routine laboratory measures capture dewatering from different angles. Canadian standard freeness (CSF), defined in TAPPI T 227, gauges how fast a dilute suspension drains through a standardized orifice and screen under gravity. CSF is sensitive to fiber swelling, surface condition, and fines content, and it also responds to practical factors such as stock preparation and temperature. Drainage time recorded during handsheet formation – using TAPPI T 205 (British/standard handsheet former) and timed per TAPPI T 221 – provides a direct measure of how quickly water leaves the forming mat under the geometry used for laboratory sheets. These two metrics reflect a common physical cause – hydrodynamic resistance – but their relationship is not strictly linear and depends on pulp type, refining history, and fines management.

Refining (beating) is the papermaker's main lever for tuning this resistance and the resulting strength–drainage balance. Through external fibrillation, internal delamination, limited cutting, and fines generation, refining increases fiber flexibility and bonding potential, enhancing tensile and burst strength, but usually lowering bulk and freeness.[1-5] The net effect on dewatering arises from competing influences: improved conformability (facilitating network consolidation) versus increased filtration resistance (slowing flow). Numerous studies document how refining intensity and specific energy shape fiber morphology, fines production, and, consequently, drainage kinetics across hardwood and softwood kraft pulps and their blends.[6-8] The consensus is clear: as refining progresses, freeness declines and drainage time rises, yet the rate and curvature of this rise are pulp-specific.

TAPPI guidance cautions against assuming a simple mapping between CSF and drainage time. The freeness tester features a short, throttled flow path dominated by an orifice, whereas the

handsheet former disperses flow through a porous fabric and a compressible, evolving mat. Differences in geometry, pressure profile, and mat development mean that the same stock can show different sensitivities in the two tests. As a result, nonlinearity and pulp specificity are expected in CSF–drainage correlations. Understanding and modeling this mapping is important for interpreting laboratory results, comparing pulps of different origin, and setting refining targets that jointly optimize drainage and strength.

A mechanistic lens for both tests is Darcy-type flow through compressible porous media. Classical analyses of drainage and wet pressing use Darcy's law and Kozeny–Carman relations to express time or flow in terms of viscosity, pressure drop, porosity, and a permeability that depends on fiber structure and fines content. The specific filtration resistance (or its inverse, permeability) is central. When this resistance is empirically tied to CSF (or to Schopper–Riegler, °SR), one naturally obtains curvilinear relations between drainage time and CSF. Over typical laboratory ranges, these relations are often well captured by hyperbolic, power-law, or log-transformed forms, depending on how permeability scales with refining-induced structure.[9,10] In a notable analysis, El-Hosseiny and Yan derived a CSF expression from pressure-filtration theory, linking the outcome to consistency, water viscosity, and intrinsic resistance.[11] Subsequent discussions clarified when screen resistance can be neglected relative to mat resistance, reinforcing a filtration-controlled view of dewatering.[12]

Beyond wood pulps, the growing industrial interest in non-wood fibers – for example, bagasse, wheat straw, and bamboo – raises practical questions about portability of CSF–time correlations. Non-wood furnishes differ in fiber dimensions, parenchyma/vessel content, silica/ash levels, and fines behavior. Many show intrinsically poorer drainage in the unrefined state and distinct refining trajectories compared to hardwood/softwood kraft.[13] For bagasse, filtration studies have quantified pad permeability and compressibility and developed one-dimensional models under pressure-filtration, emphasizing sensitivity to depithing, fractionation, and fines control.[14,15] Although the test geometries differ from a British-type former, these works support the expectation of nonlinearity and validate the use of inverse, log, or power-law empirical forms. Wheat straw often drains slowly due to high parenchyma and fines content; process reviews highlight chemical or enzymatic strategies to improve drainability, but the freeness–drainage mapping remains system-specific.[16,17] Bamboo shows its own trajectory linked to length distribution and wall structure, again arguing for empirical fits tailored by furnish family and refining level.

Across all pulp types, fines management is a key mechanistic driver for model parameters. Primary and secondary fines can accumulate near the wire and within the mat, sharply increasing specific resistance and lowering permeability. Because refining elevates fines content – and because fines characteristics vary by furnish – stocks with similar CSF can nonetheless exhibit different drainage times. In modeling terms, such differences shift fitted curves upward (higher intercepts) or alter slopes in hyperbolic or power-law forms. Mixed furnishes (*e.g.*, hardwood/softwood blends, co-refined *vs* separately refined) add further variability: energy partitioning, fines attachment, and fibrillation patterns can differ, altering dewatering response.[8,18] These considerations explain why a single universal equation rarely fits all pulps equally well and why improvements often follow from transformed regressions or multi-factor models that include, for example, consistency or temperature.

Against this background, the present evaluation focuses on a controlled, standardized handsheet protocol (TAPPI T 205) applied to five bleached pulps – hardwood, softwood, bamboo, wheat straw, and bagasse – refined over practical CSF ranges. For each pulp and refining level, the study pairs CSF (T 227) with drainage time (T 205/T 221 timing convention) and compares three compact equations that have strong empirical and mechanistic motivation: (i) Reciprocal (hyperbolic): $t = a + b/CSF$, (ii) Variance-stabilizing transform: $\sqrt{t} = a + b.\log(CSF)$, and (iii) Power-law (log-log): $\log t = a + b.\log(CSF)$ (equivalently $t = \exp(a)\, CSF^{b}$).

The novelty of this work lies in (i) applying a single formation protocol across multiple pulp classes and refining levels, and (ii) confronting three parsimonious equations on the same datasets, rather than adopting one model by tradition. Reporting RMSEE on the original scale avoids ambiguity from transformations and enables direct comparison with machine expectations (seconds). By calibrating across furnishes, the results provide both actionable correlations – to estimate drainage time from CSF within observed ranges – and

mechanistic context, linking parameter shifts to fines content, compressibility, and mat structure.

Finally, this study is aligned with current interests in sustainable papermaking and alternative fibers. As mills explore bamboo, wheat straw, and bagasse to diversify fiber supply and reduce environmental footprint, robust laboratory-scale tools for predicting drainage behavior become more valuable. Empirical mappings between CSF and handsheet drainage time, anchored in Darcy-type concepts and calibrated across furnishes, can support refining targets, chemical strategies (*e.g.*, fines control), and formation settings, helping reconcile productivity with property goals. In short, selecting an appropriate compact model – hyperbolic, √t–log(CSF), or log–log – by pulp family and refining window can improve the reliability of dewatering control, while preserving strength objectives and machine productivity.

EXPERIMENTAL

Materials and pulp sources

Five bleached cellulosic pulps representing both wood and non-wood fibers were evaluated: softwood, hardwood, bamboo, bagasse, and wheat straw. The hardwood, bamboo, and bagasse pulps were obtained from the Central Pulp and Paper Research Institute (CPPRI), Saharanpur, India. The softwood pulp was sourced from a commercial kraft pulp mill, and the wheat straw pulp was produced at laboratory scale. Upon receipt, all pulps were stored in sealed polyethylene bags at 4 °C to limit biological activity and moisture loss until use.

Pulp preparation and refining protocol

Before refining, cold-stored pulps were equilibrated to room temperature, then each pulp was slushed in deionized water to prepare a stock at 10% consistency. The furnish was homogenized by gentle mechanical agitation to minimize fiber flocculation. Refining was performed in a PFI mill in accordance with TAPPI T 248 sp-00 (Laboratory beating of pulp –PFI mill method). For every refining condition, the required number of PFI revolutions was determined from preliminary trials to reach target freeness values (see "Freeness ranges" below). The PFI mill was inspected for roll clearance and calibrated contact. Between batches of refining levels of the pulps, the mill chamber and roll were rinsed thoroughly with deionized water to avoid cross-contamination and to prevent fines carryover. The refined pulps were covered to prevent evaporation and tested within the same working day.

The initial freeness (unrefined) of the pulps was: softwood 690 mL CSF, hardwood 670 mL CSF, bamboo 710 mL CSF, bagasse 430 mL CSF, and wheat straw 400 mL CSF. Refining intensity and number of levels per pulp were chosen so that each material spanned a practically relevant interval for handsheet formation and wet-end operations: softwood, hardwood, bagasse – refined to four distinct freeness levels each; bamboo – refined to three levels; wheat straw – refined to two levels.

Across the study, the following CSF intervals were covered: softwood: 690 → 330 mL CSF; hardwood: 670 → 290 mL CSF; bamboo: 710 → 340 mL CSF; bagasse: 430 → 225 mL CSF; wheat straw: 400 → 260 mL CSF. Collectively, the dataset spans approximately 225–710 mL CSF, which encompasses freeness levels commonly encountered in approach-flow and wet-end control for a range of grades.

Freeness measurement

Immediately after refining, an aliquot was taken for CSF determination. Freeness was measured according to TAPPI T 227 om-99 (Canadian standard freeness of pulp). Measurements were carried out with temperature-equilibrated deionized water. The freeness tester was cleaned, the screens inspected, and the orifice checked for blockage prior to each measurement series. For each refined sample, at least two determinations of CSF were made; if duplicate values differed by more than 10 mL, a third determination was performed and the outlier discarded. The freeness tester's screens and orifice were verified daily. Reported CSF values are the mean of accepted replicates.

Handsheet formation and drainage time

The remainder of the refined stock was diluted for handsheet formation (T 205) and drainage time was measured during sheet formation. Drainage times were recorded during handsheet making using a standard (British-type) handsheet former operated in accordance with TAPPI T 205 sp-95 (Forming handsheets for physical tests of pulp). Sheets were formed at a basis weight of 60 g m^{-2}. The furnish was diluted to the prescribed forming consistency with deionized water and gently stirred immediately before charging the former to minimize flocculation. The drainage time was defined as the elapsed time from opening the valve (or lifting the plug) to the cessation of visible free surface water flow through the wire, following the timing convention in T 205. Stopwatch response and operator timing were verified with trial runs at the start of each session.

All tests were performed under controlled laboratory conditions (ambient 25 ± 2 °C, relative humidity 65 ± 5%). Where necessary, the temperature of process water was adjusted to reduce viscosity variability because viscosity changes can affect both CSF and drainage time. For each refined pulp level, 8 handsheets were formed; drainage time was recorded for each sheet and the mean value was used for analysis. If a reading deviated by more than 10% from the

median of the set, the test was repeated and the discrepant value investigated for procedural anomalies (*e.g.*, air entrainment, accidental loss of fines).

All dilutions used deionized water to avoid ionic strength effects that could alter swelling or flocculation. Slurry consistency at refining, freeness measurement, and sheet formation was verified gravimetrically (oven-dry solids at 105 °C). For each CSF level per pulp, the mean CSF and the mean drainage time (seconds) were entered into the modeling dataset.

Data analysis and curve fitting

The relationship between drainage time (t) and freeness (CSF) was evaluated with three compact models that are commonly used to capture the nonlinearity observed in dewatering data: (i) Reciprocal (hyperbolic): $t = a + b.CSF$ (ii) Square-root/log transform: $\sqrt{t} = a + b.\log(CSF)$ (iii) Power-law (log–log): $\log t = a + b.\log(CSF) \Leftrightarrow t = \exp(a).CSF^{b}$

For models (ii) and (iii), regressions were performed in the transformed space. To enable comparison on a common physical basis, predictions were back-transformed to seconds before computing all performance metrics. Goodness of fit was quantified by the coefficient of determination R^2 and the root mean square error of estimate (RMSEE) on the original time scale (seconds). With multiple handsheet replicates available at a given CSF, the mean drainage time was used as the response value. Residual plots (predicted *vs* residual; residual *vs* CSF) were inspected for curvature, heteroscedasticity, or outliers.

To reduce bias from differing CSF ranges among pulps, all fits were performed separately for each pulp across its refined levels (*e.g.*, softwood 690–330 mL; wheat straw 400–260 mL). This avoids conflating across-pulp structural differences (fiber length distribution, fines generation, parenchyma content, *etc*.) with within-pulp refining effects. Comparative assessment focused on (i) which of the three forms minimized RMSEE for a given pulp, and (ii) whether a single form consistently dominated across wood and non-wood pulps.

Because CSF and drainage time originate from different measurement geometries, their mapping can be apparatus-specific. Although we adhered strictly to TAPPI T 227 and T 205, small differences in former design, valve response, and operator timing can influence absolute drainage times. Therefore, all comparisons were made within this study's standardized setup, and the models are intended to describe behavior over the specific CSF ranges tested for each pulp. Extending predictions far outside the observed ranges (*e.g.*, to very low CSF for wheat straw or very high CSF for bamboo) should be done cautiously and preferably validated with additional experiments.

RESULTS AND DISCUSSION

Based on the refining experiments, the data on pulp freeness and drainage time were analysed through some typical tables and plots based on three compact models. The next sections describe what the results mean, compare how refining affects the different pulps, and show which curve best fits the drainage time and freeness.

Effect of refining on freeness and drainage time of pulps

Refining decreases CSF (poorer freeness) by increasing external fibrillation, internal swelling, and fines generation. In a British/standard handsheet former, this structural change raises the mat's specific filtration resistance, so drainage time increases as freeness declines. In Figure 1, every pulp follows this qualitative trend; what differs is how quickly drainage time rises (the slope/curvature) and the absolute level at comparable freeness. Drainage time varied from one pulp to another. It was found as Wheat straw > Baggase > Hardwood > Bamboo > Softwood. These differences reflect fiber morphology (length, coarseness, wall thickness), fines and parenchyma content, vessel/pith fragments, and how each pulp responds to PFI refining.

Compared to softwood, hardwood fibers are shorter and often generate fines more readily at a given energy, but their starting freeness is also high. In Figure 1, hardwood's curve is monotonic and typically less steep than the non-wood pulps over the same CSF window, indicating that while fines accumulation slows drainage, the hardwood mat does not become resistant as quickly as straw/bagasse mats. As refining progresses, the drainage time of softwood pulp increases; however, the increase is not markedly sharper than that of hardwood at comparable reductions in CSF. Due to the longer fiber length and higher aspect ratio, softwood initially forms a relatively open fiber mat under light refining conditions. Since the results do not quantify fines generation or fiber fibrillation, it cannot be conclusively stated that significant fines production or extensive fibrillation led to any pronounced acceleration in drainage time. Relative to hardwood/softwood, bamboo's curve commonly shows greater

sensitivity once CSF passes below the mid-range. Wheat straw exhibits a steeper drainage-time increase with decreasing CSF than wood pulps. Even at moderate refining, Figure 1 shows wheat straw's drainage time rising faster per unit CSF loss, signaling a rapid build-up of hydraulic resistance.

Bagasse shows one of the steepest rises in drainage time as CSF declines. In Figure 1, the curve climbs quickly over the studied range, and at low CSF the drainage times are among the highest across all pulps.

Wood pulps (softwood, hardwood) offer more forgiving refining windows, while bamboo displays a mid-range sensitivity that warrants careful control. Wheat straw and bagasse incur steeper drainage penalties, reflecting fines-rich microstructures that rapidly reduce permeability as refining proceeds. These distinctions matter directly for handsheet preparation and scale-up to machine trials: they guide refining set-points, consistency targets, vacuum capacity, and chemical programs needed to balance strength development against dewatering capacity.

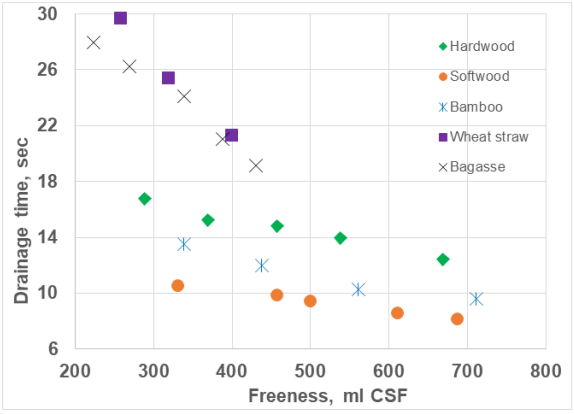

Figure 1: Effect of refining of different pulps: (a) hardwood, (b) softwood, (c) bamboo, (d) wheat straw, (e) bagasse, on drainage time during handsheet making

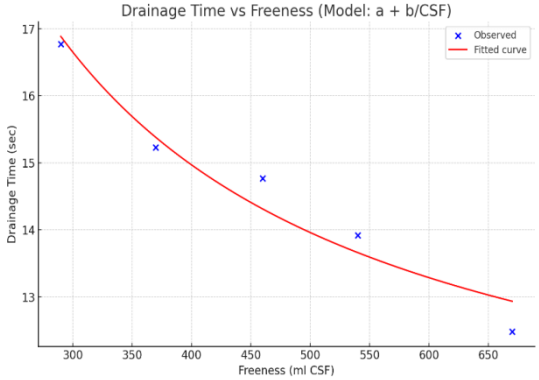

Figure 2: The fitted curve against observed data as per hyperbolic (reciprocal) model for hardwood pulp

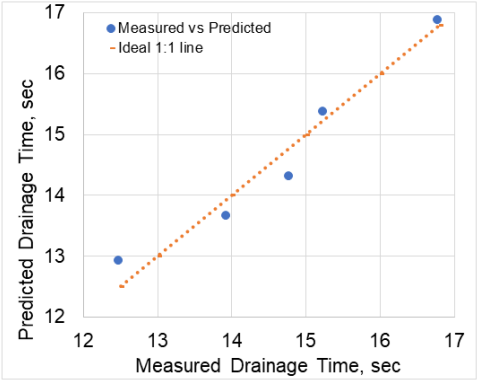

Figure 3: Measured drainage time *vs.* predicted drainage time as per hyperbolic (reciprocal) model for hardwood pulp

Table 1
Summary of drainage time fits (Drainage time = a + b/CSF) for different pulps

Pulp	a	b	R^2	RMSEE
Hardwood	9.919	2020.233	0.948	0.322
Softwood	6.119	1522.940	0.940	0.211
Bamboo	5.871	2614.972	0.991	0.142
Wheat straw	5.490	6327.756	0.999	0.117
Bagasse	10.841	4023.849	0.924	0.903

Table 2
Measured *vs*. predicted drainage times, with both absolute and percentage errors for different pulps

Pulp	Freeness (mL CSF)	Measured time (s)	Predicted time (s)	Error (measured - predicted)	% Error
Hardwood	670	12.48	12.934	-0.454	-3.64
	540	13.92	13.660	0.260	1.87
	460	14.77	14.311	0.459	3.11
	370	15.23	15.379	-0.149	-0.98
	290	16.77	16.885	-0.115	-0.69
Softwood	690	8.13	8.326	-0.196	-2.41
	610	8.53	8.616	-0.086	-1.00
	500	9.29	9.165	0.125	1.35
	460	9.78	9.430	0.350	3.58
	330	10.54	10.734	-0.194	-1.84
Bamboo	710	9.64	9.554	0.086	0.89
	560	10.33	10.541	-0.211	-2.04
	440	11.98	11.814	0.166	1.38
	340	13.52	13.562	-0.042	-0.31
Wheat straw	400	21.22	21.309	-0.089	-0.42
	320	25.43	25.264	0.166	0.65
	260	29.75	29.828	-0.078	-0.26
Bagasse	430	19.11	20.199	-1.089	-5.70
	390	21.03	21.159	-0.129	-0.61
	340	24.14	22.676	1.464	6.07
	270	26.21	25.744	0.466	1.78
	225	28.01	28.725	-0.715	-2.55

Model (ii) $\sqrt{t} = a + b.log\ (CSF)$

Fit quality and parameters

Figures were drawn displaying the variance-stabilizing log/√ transformation (√(Drainage time) = a + b.log(CSF)) fits alongside the observed freeness-drainage time data for five pulp types: (a) hardwood, (b) softwood, (c) bamboo, (d) wheat straw, (e) bagasse; and as an illustration the fitted curve for hardwood pulp is presented in Figure 4. The variance-stabilizing model √t = a + b.log(CSF) captures curvature effectively across pulps. Fits improve notably for non-woods: wheat straw approaches a perfect overlay, while bagasse residuals narrow *versus* the hyperbola. Hardwood, softwood, and bamboo also show tighter alignment, especially in mid-to-low CSF regions where variance typically expands. Table 3 summarizes the drainage time fits for each pulp, reporting the corresponding values of a, b, R^2, and RMSEE. The R^2 value was improved or comparable to the reciprocal form for all pulps (0.950–0.999). Notably, wheat straw achieved ~1.000 (0.9999). This could be also because only three data points for wheat straw were used to apply mathematical models to fit these three measured points. With so few experimental results, the mathematical model can give a perfect fit. The RMSEE values overall appeared here with the lowest errors for several pulps− wheat straw: 0.014 s (near-perfect fit), bamboo: 0.195 s, hardwood: 0.238 s, softwood: 0.139 s, and bagasse: 0.728 s (still higher than others, but better than the reciprocal model). In Table 4, results from the √t–log(CSF) variance-stabilizing fit are shown, listing measured and predicted drainage times and the corresponding absolute and percentage errors for each pulp. Compared to the reciprocal model, the error ranges (%) tightened for most pulps; *e.g*., hardwood narrowed to −1.83% to +2.12%, softwood to −1.48% to +2.51%, bamboo to −2.92% to +2.23%, wheat straw to −0.08% to +0.03%, and bagasse to −3.84% to +5.35%. The measured and predicted drainage times for each pulp were compared using the √t–log(CSF) model and as an illustration the fitted curve for hardwood pulp is presented in Figure 5. Measured–predicted comparisons under the √t–log(CSF) formulation show tightened scatter around the 1:1 line. Wheat straw points align almost exactly; hardwood, softwood, and bamboo are close with minimal spread. Bagasse improves relative to the hyperbola, but still displays the widest dispersion, consistent with fines/pith effects.

The √t vs log(CSF) transformation stabilizes variance and captures curvature well, delivering the tightest predictions for wheat straw and a clear

improvement for bagasse relative to the reciprocal form.

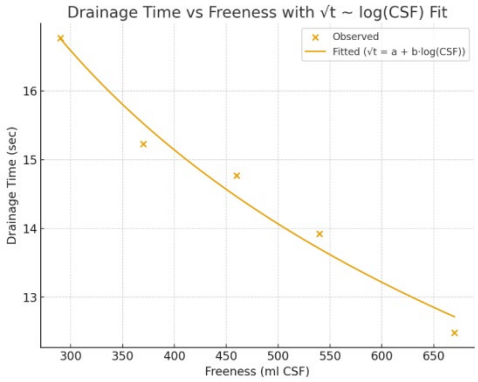

Figure 4: The fitted curve against observed data as per variance-stabilizing log/√ transformation for hardwood pulp

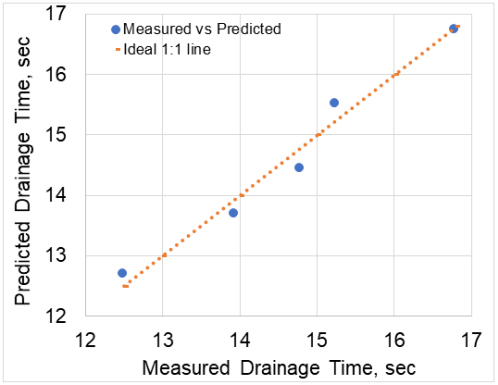

Figure 5: Measured drainage time *vs.* predicted drainage time as per variance-stabilizing log/√ transformation for hardwood pulp

Table 3
Summary of drainage time fits (√(Drainage time) = a + b.Log (CSF)) for different pulps

Pulp	a	b	R^2	RMSEE
Hardwood	7.671	-0.631	0.972	0.238
Softwood	6.460	-0.550	0.974	0.139
Bamboo	8.342	-0.803	0.983	0.195
Wheat straw	16.397	-1.968	0.999	0.014
Bagasse	12.853	-1.385	0.950	0.728

Table 4
Measured *vs*. predicted drainage times, with both absolute and percentage errors for different pulps

Pulp	Freeness (mL CSF)	Measured time (s)	Predicted time (s)	Error (measured - predicted)	% Error
Hardwood	670	12.48	12.709	-0.234	-1.83
	540	13.92	13.698	0.217	1.60
	460	14.77	14.457	0.308	2.12
	370	15.23	15.520	-0.296	-1.91
	290	16.77	16.755	0.009	0.09
Softwood	690	8.13	8.207	-0.072	-0.95
	610	8.53	8.600	-0.065	-0.82
	500	9.29	9.254	0.041	0.39
	460	9.78	9.535	0.250	2.51
	330	10.54	10.696	-0.151	-1.48
Bamboo	710	9.64	9.425	0.197	2.23
	560	10.33	10.632	-0.320	-2.92
	440	11.98	11.932	0.030	0.40
	340	13.52	13.406	0.096	0.85
Wheat straw	400	21.22	21.213	0.009	0.03
	320	25.43	25.451	-0.019	-0.08
	260	29.75	29.742	0.011	0.03
Bagasse	430	19.11	19.844	-0.748	-3.84
	390	21.03	21.067	-0.051	-0.18
	340	24.14	22.848	1.278	5.35
	270	26.21	26.002	0.194	0.79
	225	28.01	28.641	-0.645	-2.25

Model (iii) $\log t = a + b.log\,(CSF)$ — Fit quality and parameters

The measured freeness–drainage time points were plotted together with the corresponding log–log (power-law) model curves (logt = a + b.log(CSF)) for each pulp: hardwood, softwood, bamboo, wheat straw, and bagasse. The fitted curve for hardwood pulp is presented in Figure 6 as an illustration. Power-law (log–log) fits log t = a + b.log(CSF) provide a broad-range description of drainage behaviour. The curvature in bamboo and non-woods is well represented, while wood pulps remain well fitted across their ranges. Parameter differences reflect pulp-specific sensitivity of drainage time to freeness changes, especially as CSF approaches lower values. The fitted drainage time parameters (a and b) and performance metrics (R^2, RMSEE) for each pulp are compiled in Table 5. The R^2 values were very strong fit overall (0.939–0.999). Wheat straw again near-perfect at 0.9996; bamboo at 0.987; hardwood/softwood around 0.968–0.968; bagasse lowest at 0.939. The RMSEE was the best (smallest) for wheat straw (0.089 s), competitive for bamboo (0.170 s) and softwood (0.155 s). Hardwood sat at 0.252 s; bagasse remained highest at 0.806 s.

Table 6 summarizes, for each pulp, the measured and modeled drainage times under the log–log (power-law) approach, including both absolute and percentage error values.

Compared to √t–log model, the error ranges (%) for most pulps were: hardwood -2.12% to +2.28%, softwood −1.65% to +2.83%, bamboo −2.86% to +1.53%, wheat straw −0.004% to +0.60%. Bagasse remained the most challenging (−4.11% to +5.73%). As an illustration, Figure 7 displays the match between measured and predicted drainage times under the log–log (power-law) model for hardwood pulp. Predicted versus measured plots for the log–log model show strong agreement across all pulps, rivaling the √t−log(CSF) performance. Wheat straw and bamboo exhibit tight clustering; hardwood and softwood remain close to the 1:1 line. Bagasse retains the largest spread but with reduced bias compared to the reciprocal model.

The log–log power law competes closely with the √t–log form, especially for wheat straw and bamboo; it also gives stable performance for softwood and hardwood. For bagasse, improvements are visible *vs* the reciprocal model, but not as dramatic as for wheat straw.

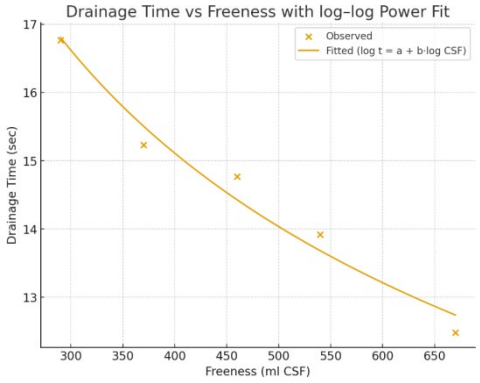

Figure 6: The fitted curve against observed data as per power-law (log–log) model for hardwood pulp

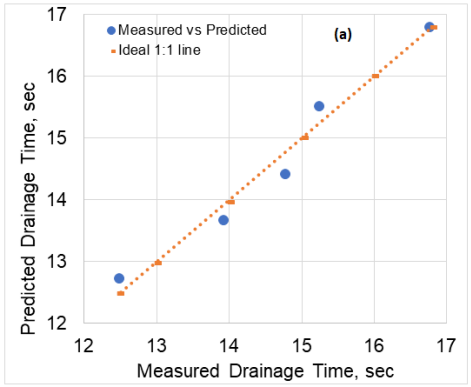

Figure 7: Measured drainage time *vs*. predicted drainage time as per power-law (log–log) model for hardwood pulp

Table 5
Summary of drainage time fits (log(drainage time) = a + b.log(CSF)) for different pulps

Pulp	a	b	R^2	RMSEE
Hardwood	4.699	-0.331	0.968	0.252
Softwood	4.465	-0.361	0.968	0.155
Bamboo	5.369	-0.475	0.987	0.170
Wheat straw	7.758	-0.785	0.999	0.089
Bagasse	6.459	-0.572	0.939	0.806

Table 6
Measured *vs.* predicted drainage times, with both absolute and percentage errors for different pulps

Pulp	Freeness (mL CSF)	Measured time (s)	Predicted time (s)	Error (measured - predicted)	% Error
Hardwood	670	12.48	12.744	-0.264	-2.12
	540	13.92	13.688	0.232	1.67
	460	14.77	14.434	0.336	2.28
	370	15.23	15.512	-0.282	-1.85
	290	16.77	16.815	-0.045	-0.27
Softwood	690	8.13	8.209	-0.079	-0.97
	610	8.53	8.583	-0.053	-0.62
	500	9.29	9.221	0.069	0.74
	460	9.78	9.503	0.277	2.83
	330	10.54	10.714	-0.174	-1.65
Bamboo	710	9.64	9.492	0.148	1.53
	560	10.33	10.625	-0.295	-2.86
	440	11.98	11.915	0.065	0.54
	340	13.52	13.467	0.053	0.39
Wheat straw	400	21.22	21.215	-0.005	-0.024
	320	25.43	25.276	0.154	0.60
	260	29.75	29.751	-0.001	-0.004
Bagasse	430	19.11	19.896	-0.783	-4.11
	390	21.03	21.039	-0.006	-0.04
	340	24.14	22.756	1.387	5.73
	270	26.21	25.964	0.250	0.94
	225	28.01	28.818	-0.804	-2.88

Measured *vs.* predicted performance

Across models, pointwise errors stay within a few percent for hardwood, softwood, bamboo, with wheat straw being exceptionally tight (errors typically within ±0.65%, and even ±0.004% for the √t–log model). Bagasse shows the largest pointwise deviations (up to ~±6.07%) – most notably around CSF ≈ 340 mL, where each model tends to under- or over-predict by ~5–6% (Tables 2, 4, and 6). These tables confirm that the choice of transformation matters: for the same datapoints, √t–log and log–log reduce systematic deviation more effectively than the reciprocal model, especially for non-woods.

Head-to-head comparison by pulp

For hardwood, all three models performed well (R^2 ≈ 0.948–0.972; RMSEE ≈ 0.24–0.32 s). The tightest error ranged under √t–log (−1.91% to +2.12%) and log–log (−2.12% to +2.28%), slightly better than the reciprocal model (−3.64% to +3.11%) (Table 7). So, either √t–log or log–log edges out the reciprocal model for accuracy.

For softwood, strong fits observed across all models (R^2 ≈ 0.940–0.974). The lowest RMSEE with (0.139 s), and narrow error ranges (−1.48% to +2.51%) were observed with √t–log model. So, √t–log offers the best overall accuracy; log–log was close.

For bamboo, high R^2 in every model (≈ 0.983–0.991). The √t–log and log–log both delivered small RMSEE (~0.19–0.17 s) and tight error ranged (roughly ±2–3%); reciprocal was also excellent with slightly lower RMSEE.

For wheat straw, near-perfect fits in all transformed models: R^2 ≈ 0.9996–0.9999; RMSEE stunningly low (0.014–0.117 s). Errors were essentially negligible for √t–log (−0.08% to +0.03%) and very small for log–log (−0.004% to +0.60%); reciprocal was also excellent but slightly larger (−0.42% to +0.65%). So, √t–log provides the best match for wheat straw, with log–log a close second.

For bagasse, lowest R^2 among pulps across models (0.924–0.950), largest RMSEE values (0.728–0.903 s), and widest %-error ranges (up to ±6%). Even so, √t–log and log–log improve RMSEE and narrow the error spread compared with the reciprocal model. So, bagasse remained the most challenging system to predict; transformed models help, but residuals probably indicate additional structure (*e.g.*, fines/pith

effects) not captured by single-parameter curvature alone.

Table 7
Comparison of percentage errors (measured *vs*. predicted drainage times) for different pulps

Pulp	% Error (measured *vs* predicted)		
	Drainage time = a + b/CSF	√(Drainage time) = a + b.Log (CSF)	log(drainage time) = a + b.log(CSF)
Hardwood	(-3.64 to 3.11)	(-1.91 to 2.12)	(-2.12 to 2.28)
Softwood	(-2.41 to 3.58)	(-1.48 to 2.51)	(-1.65 to 2.83)
Bamboo	(-2.04 to 1.38)	(-2.92 to 2.23)	(-2.86 to 1.53)
Wheat straw	(-0.42 to 0.65)	(-0.08 to 0.03)	(-0.004 to 0.60)
Bagasse	(-5.70 to 6.07)	(-3.84 to 5.35)	(-4.11 to 5.73)

Overall takeaways across all models and pulps

All three model forms captured the inverse relation between freeness (CSF) and drainage time: as CSF decreased (more refining), drainage time increased. Non-wood pulps (wheat straw, bagasse) showed higher absolute drainage times and generally steeper sensitivity to CSF changes than wood pulps, which was reflected in their fit parameters and error behavior. Among the three models, the √t vs log(CSF) and log–log forms often yielded equal or better R^2 and lower RMSEE than the simple reciprocal model, particularly for pulps exhibiting stronger curvature (*e.g*., wheat straw, bagasse).

For wood pulps (hardwood, softwood), all models are serviceable; the √t–log or log–log forms provide modest but consistent accuracy gains. For bamboo, the reciprocal model should be selected instead of log–log or √t–log for best point predictions. For wheat straw, the √t–log model is clearly preferred, producing virtually zero bias over the tested range. For bagasse, higher uncertainty should be expected, and √t–log or log–log should be used instead of the reciprocal form. Taken together, the results suggest that the tested drainage models are broadly effective across a diverse set of pulps, with especially strong performance for wheat straw, bamboo, hardwood, and softwood. Bagasse remains the main outlier, showing higher error and weaker model fit.

CONCLUSION

Refining consistently decreased freeness and increased drainage time for all pulps, but sensitivity to refining differed by fiber family. Wood pulps (hardwood, softwood) showed moderate, smooth increases and were well captured by all models, with slight advantages for the transformed forms. Bamboo displayed stronger curvature as refining progressed, favoring √t-log(CSF) or log–log fits. Wheat straw produced exceptionally tight predictions with the √t-log(CSF) model, indicating that variance stabilization and a logarithmic CSF term suit its drainage response. Bagasse exhibited the largest errors across models, implying additional structure (*e.g*., fines/pith distribution, compressibility) not explained by CSF alone. Practically, the transformed models provide more robust prediction across pulps, but model selection should be tailored: √t-log(CSF) for straw (and often softwood), either transformed option for hardwood and reciprocal model for bamboo.

ACKNOWLEDGEMENTS: Acknowledgements are due to Mr. Hussen Naik Banavath for executing the experimental work and to Dr. Sanjay Tyagi, Senior Scientist, Central Pulp and Paper Research Institute, Saharanpur, for providing pulp samples and valuable help during experimentation.

REFERENCES

[1] H. N. Banavath, N. K. Bhardwaj and A. K. Ray, *IPPTA J*., **21**, 141 (2009)
[2] H. N. Banavath, N. K. Bhardwaj and A. K. Ray, *Bioresour. Technol*., **102**, 4544 (2011), https://doi.org/10.1016/j.biortech.2010.12.109
[3] V. Kumar, P. Pathak and N. K. Bhardwaj, *Cellulose Chem. Technol*., **56**, 625 (2022), https://doi.org/10.35812/CelluloseChemTechnol.2022.56.55
[4] N. K. Bhardwaj, *Cellulose Chem. Technol*., **53**, 113 (2019), https://doi.org/10.35812/CelluloseChemTechnol.2019.53.13
[5] N. K. Bhardwaj, V. Hoang and K. L. Nguyen, *Bioresour. Technol*., **98**, 1647 (2007)
[6] J. H. Ryu, C. H. Kim, J. Y. Lee, J. S. Lee, C. H. Lee *et al*., *Appl. Sci*., **12**, 11445 (2022), https://doi.org/10.3390/app122211445
[7] K. Koskenhely, A. Ämmälä, H. Jokinen and H. Paulapuro, in "Advances in Paper Science and

Technology, Trans. XIII[th] Fund. Res. Symp. Cambridge, 2005", edited by S. J. I'Anson, FRC, Manchester, 2018, pp. 427–456, https://doi.org/10.15376/frc.2005.1.427
[8] S. Panthai and P. Somboon, *Kasetsart J.* (*Nat. Sci.*), **48**, 540 (2014)
[9] J. D. McDonald and R. J. Kerkes, *BioResources*, **12**, 9520 (2017)
[10] K. Kalliokoski, Master of Science Thesis, University of Oulu, Faculty of Technology, Department of Electrical and Information Engineering, 2011
[11] F. El-Hosseiny and J. F. Yan, *Pulp Pap. Can.*, **81**, T113 (1980)
[12] P. C. Swodzinski and M. R. Doshi, *Mathematical Models of Canadian Standard Freeness (CSF) and Schopper-Riegler Freeness (SR)*, IPC Technical Paper Series No. 172, The Institute of Paper Chemistry, Appleton, Wisconsin, 1986
[13] T. Ferdous, Y. Ni, M. A. Quaiyyum, M. N. Uddin and M. S. Jahan, *ACS Omega*, **6**, 21613 (2021), https://doi.org/10.1021/acsomega.1c02933
[14] T. J. Rainey, W. O. S. Doherty, D. M. Martinez, R. J. Brown and N. A. Kelson, *Transp. Por. Media*, **86**, 737 (2011), https://doi.org/10.1007/s11242-010-9649-x
[15] T. J. Rainey, Ph.D. Thesis, Queensland University of Technology, 2009
[16] H. Zhang, J. Li, H. Hu, Z. He and Y. Ni, *Bioresour. Technol.*, **120**, 40 (2012), https://doi.org/10.1016/j.biortech.2012.06.008
[17] F. Urdaneta, L. Meza, R. Márquez, J. Franco, R. E. Vera *et al.*, *Cellulose*, **32**, 5021 (2025), https://doi.org/10.1007/s10570-025-06529-4
[18] V. S. Chauhan, N. Kumar, M. Kumar, S. K. Chakrabarti and S. K. Thapar, *J. Korea TAPPI*, **43**, 142 (2011)